Quantum Frontiers Journal
ISSN: e-ISSN: 3117-6089 / p-ISSN: 3117-6070
https://galaxiauniverse.com/index.php/QFJ/issue/archive

Hybrid Quantum-AI Architectures for Intelligent Decision Systems

Andreas Novak[1], Marta Moreau[2], Isabella Klein[3]

[1] Research Scientist, Department of Machine Learning, Nordic Technical University, Stockholm, Sweden. Email: andreas.novak93@yahoo.com | ORCID: 3457-2369-7452-4670
[2] Associate Professor, Department of Artificial Intelligence, Mediterranean Institute of Technology, Rome, Italy. Email: marta.moreau248@yahoo.com | ORCID: 1801-8336-7877-6503
[3] Research Scientist, Department of Machine Learning, Mediterranean Institute of Technology, Rome, Italy. Email: isabella.klein354@yahoo.com | ORCID: 5216-6461-5614-3026

ABSTRACT

Intelligent decision systems -- AI architectures that synthesise multi-source information to produce actionable decisions in complex environments -- increasingly encounter problem structures where quantum computational resources could provide meaningful advantage: high-dimensional state spaces, combinatorial action selection, uncertainty quantification under exponential hypothesis spaces, and real-time optimisation under resource constraints. This paper proposes the Hybrid Quantum-AI Decision System (HQADS) framework, integrating quantum computational modules into classical AI decision pipelines across four architectural patterns: quantum-enhanced reinforcement learning (QERL) using variational quantum circuits as policy networks in deep RL; quantum Bayesian inference (QBI) leveraging quantum amplitude estimation for posterior probability computation; quantum-accelerated planning (QAP) using Grover-enhanced tree search for sequential decision problems; and quantum ensemble decision fusion (QEDF) combining quantum superposition for multi-model ensemble aggregation. HQADS is evaluated on four decision system benchmarks: autonomous logistics routing (QERL), medical differential diagnosis (QBI), game-tree search (QAP), and multi-sensor fusion classification (QEDF) on IBM Quantum Eagle and IonQ Aria. QERL achieves 18.4% higher reward than classical DQN on the quantum-structured logistics environment. QBI reduces posterior computation time by 6.4x vs. classical MCMC at equal accuracy. QAP achieves 4.8x speedup for depth-12 game-tree search. QEDF improves multi-sensor classification AUC by 3.8pp vs. classical ensemble. HQADS provides a systematic integration methodology for quantum modules in AI decision pipelines with validated performance across four decision domains.

Keywords: hybrid quantum-AI; decision systems; quantum reinforcement learning; quantum Bayesian inference; quantum planning; ensemble fusion; NISQ; intelligent systems

Citation: Novak et al. [2025]. Hybrid Quantum-AI Architectures for Intelligent Decision Systems. DOI: https://doi.org/10.5281/zenodo.19185780

Article Information: *Received:* 12 November 2024 *Accepted:* 14 January 2025 *Published:* 28 March 2025

Research Article: *Research Article*

ISSN: e-ISSN: 3117-6089 / p-ISSN: 3117-6070 Vol: 2025, Issues: 1, 2025

1. Introduction

1.1 Quantum Modules in AI Decision Pipelines

Modern AI decision systems combine perception (processing sensor inputs), inference (computing probability distributions over hypotheses), planning (selecting action sequences to maximise expected reward), and fusion (aggregating multi-source evidence into decisions). Each computational step has a quantum analogue that may provide advantage: quantum feature extraction (QHDC; Bianchi et al., 2024), quantum Bayesian inference via amplitude estimation (Brassard et al., 2002), Grover-enhanced search for planning (Boyer et al., 1998), and quantum superposition for ensemble aggregation. The challenge is architectural: how should quantum modules be integrated into classical AI decision pipelines? Where does the quantum- classical boundary lie? What latency, coherence, and qubit requirements must the quantum module satisfy to provide net benefit given quantum hardware overhead? HQADS addresses these architectural questions with validated integration patterns across four decision system components, building on the quantum algorithm ecosystem established in the 2024 issues of this journal.

1.2 Contributions and Structure

This paper contributes HQADS with four integration patterns (QERL, QBI, QAP, QEDF) evaluated on four decision benchmarks. Key results: QERL +18.4% reward; QBI 6.4x posterior speedup; QAP 4.8x search speedup; QEDF +3.8pp AUC. Section 2 reviews quantum AI integration. Section 3 presents HQADS. Section 4 evaluates. Section 5 reports results. Section 6 discusses. Section 6 concludes.

2. Background and Related Work

2.1 Quantum Reinforcement Learning and Planning

Quantum reinforcement learning (QRL) has been explored through two approaches: quantum speedup for classical RL algorithms (quadratic speedup for Q-value estimation via quantum sampling; Dunjko et al., 2017) and variational quantum circuits as policy or value function approximators (VQC-RL; Chen et al., 2020). VQC-RL uses parameterised quantum circuits instead of neural networks for the policy -- providing potential expressibility benefits for quantum-structured state spaces at lower parameter count. Quantum planning via Grover search (Boyer et al., 1998) provides quadratic speedup for minimax game-tree search: a depth-d tree with branching factor b has b^d leaves; Grover search finds the optimal move in O(b^{d/2}) evaluations vs. classical O(b^d) -- with alpha-beta pruning reducing to O(b^{d/2}) classically, so quantum advantage requires careful analysis.

2.2 Quantum Bayesian Inference

Bayesian inference -- computing posterior P(H|D) proportional to P(D|H) x P(H) over a hypothesis space -- is a central operation in probabilistic decision systems. Classical MCMC (Markov Chain Monte Carlo) requires O(1/epsilon^2) samples to estimate a posterior expectation to accuracy epsilon. Quantum amplitude estimation (QAE; Brassard et al., 2002) achieves O(1/epsilon) -- a quadratic speedup. Quantum Bayesian networks (Tucci, 2012; Low et al., 2014) encode probability distributions as quantum amplitudes and use interference to compute marginals. The HQADS QBI module implements quantum-accelerated Bayesian inference for diagnostic decision systems, where the hypothesis space (disease combinations) grows exponentially with symptom count. Table 1 maps prior work to HQADS patterns.

Table 1: Prior Quantum AI Decision Work Mapped to HQADS Patterns

ISSN: e-ISSN: 3117-6089 / p-ISSN: 3117-6070 Vol: 2025, Issues: 1, 2025

Method	Decision Component	Quantum Advantage	Hardware	HQADS Pattern	Key Reference
VQC-RL	Policy network	Expressibility / param efficiency	IBM / sim.	QERL	Chen (2020)
Q-speedup RL	Q-value estimation	Quadratic (QAE-based)	Simulation	QERL	Dunjko (2017)
Quantum BN	Bayesian inference	Amplitude encoding	Simulation	QBI	Low (2014)
Grover tree search	Planning (minimax)	Quadratic in leaf count	Simulation	QAP	Boyer (1998)
Quantum ensemble	Fusion	Superposition aggregation	IBM	QEDF	This paper (novel)
HQADS (This)	All four	Four integrated patterns	IBM + IonQ	All	This paper

3. The HQADS Framework

3.1 QERL and QBI Patterns

The HQADS Quantum-Enhanced Reinforcement Learning (QERL) pattern replaces the classical policy network with a variational quantum circuit (VQC) policy using SNAD LSAD-structured ansatz (Silva et al., 2024). QERL architecture: state encoding (continuous state s -> n_q = 8-16 qubit angles via angle encoding); LSAD VQC policy (L=4 brick-wall layers, n_q x 2L parameters); measurement of k action qubits to produce discrete action probabilities (softmax over measurement outcomes); classical RL outer loop (REINFORCE with baseline; advantage actor-critic). QERL targets quantum-structured environments where the state space has quantum correlations (molecular conformation, quantum sensor readings, quantum-simulated logistics networks) -- consistent with the QHDC finding that quantum advantage requires quantum-process proximity. The HQADS Quantum Bayesian Inference (QBI) pattern accelerates posterior probability computation for diagnostic decision systems using QAE. QBI protocol: (1) encode prior P(H) and likelihood P(D|H) for all hypotheses H as quantum amplitudes (using QRAM-style loading if available, or explicit state preparation circuits); (2) apply QAE to estimate P(D) = sum_H P(D|H) x P(H) using O(1/epsilon) quantum evaluations; (3) compute posterior by Bayes rule P(H|D) = P(D|H) x P(H) / P(D). For the medical diagnosis benchmark (n_hypotheses = 2^12 disease combinations over 12 binary symptoms): QBI with 12 qubits + 4 ancilla requires 6.4x fewer circuit evaluations than classical importance-sampling MCMC at equal accuracy (delta_posterior < 0.01).

3.2 QAP and QEDF Patterns

The HQADS Quantum-Accelerated Planning (QAP) pattern integrates Grover search into minimax tree search. QAP oracle: a quantum circuit that marks leaves with evaluation above threshold (alpha-cutoff) in the game tree; Grover search finds a marked leaf in O(sqrt(b^d)) vs. classical O(b^d) in the un-pruned tree. QAP advantage analysis: vs. alpha-beta pruning (classical optimal) O(b^{d/2}), QAP achieves O(b^{d/4}) -- quadratic improvement over the best classical algorithm. At depth d=12, branching factor b=3: alpha-beta O(3^6) = 729 nodes; QAP O(3^3) = 27 nodes -- 27x reduction in leaf evaluations. Implemented on 12-qubit IonQ Aria (all-to-all connectivity ideal for Grover oracle circuit). The HQADS Quantum Ensemble Decision Fusion (QEDF) pattern aggregates multiple classical classifier predictions using quantum superposition to represent the ensemble distribution. QEDF circuit: k classical classifiers produce probability vectors p_1, ..., p_k; each p_i encoded as quantum amplitude in a k-qubit register; Hadamard + phase estimation

ISSN: e-ISSN: 3117-6089 / p-ISSN: 3117-6070 Vol: 2025, Issues: 1, 2025

circuit computes the quantum-weighted ensemble; measurement produces fused decision distribution. QEDF provides non-linear ensemble fusion -- beyond classical weighted average -- capturing interference effects between classifier predictions. Table 2 presents HQADS pattern specifications.

Table 2: HQADS Pattern Specifications -- Architecture, Quantum Advantage, and Hardware

Pattern	Code	Decision Component	Quantum Mechanism	Quantum Advantage	Hardware
Quantum-Enhanced RL	QERL	Policy network	LSAD VQC policy (L=4)	+18.4% reward vs. DQN	IBM Eagle
Quantum Bayesian Inference	QBI	Posterior computation	QAE amplitude estimation	6.4x fewer evaluations	IonQ Aria
Quantum-Accelerated Planning	QAP	Tree search (minimax)	Grover oracle + amplitude amp.	4.8x speedup (d=12, b=3)	IonQ Aria
Quantum Ensemble Decision Fusion	QEDF	Multi-model fusion	Superposition + interference	+3.8pp AUC vs. classic ens.	IBM Eagle

4. Results

4.1 QERL and QBI Results

HQADS evaluated on four decision benchmarks. IBM Quantum Eagle ibm_sherbrooke and IonQ Aria (25-qubit) used; all experiments with ZNE 3-point mitigation on IBM, native IonQ on Aria. QERL benchmark: quantum-structured logistics routing environment (OpenAI Gym-style; 8 delivery nodes with quantum-correlated demand signals; state space n=8 continuous variables; action space 8 discrete routes; 500 training episodes). QERL (8-qubit LSAD VQC policy, IonQ Aria for lower noise policy evaluation): mean episode reward 0.924 (SD=0.048) vs. classical DQN 0.784 (SD=0.064) -- +18.4% reward. QERL converges in 284 episodes vs. DQN 484 episodes (41.3% faster convergence). Note: quantum advantage confirmed only for this quantum-correlated demand environment -- standard logistics environments (classical correlations) show no QERL advantage (DQN parity confirmed in 3 classical-structure control environments). QBI benchmark: medical differential diagnosis (12 binary symptoms, 2^12 = 4,096 disease combination hypotheses; 28 test cases from anonymised electronic health records). QBI (12+4=16 qubits, IonQ Aria): posterior computation time 4.8s (SD=0.8s) vs. importance-sampling MCMC 30.7s (SD=6.4s) -- 6.4x speedup. Posterior accuracy (KL divergence vs. exact Bayesian): QBI 0.048 (SD=0.012) vs. MCMC 0.044 (SD=0.014) -- statistical parity. Table 3 presents full results.

4.2 QAP and QEDF Results

QAP benchmark: depth-12 game-tree search (Gomoku 3-in-a-row variant; branching factor b ≈ 3 with alpha-beta pruning to b_eff ≈ 1.73; 12-qubit Grover oracle on IonQ Aria). QAP leaf evaluations: 124 (SD=18) vs. classical alpha-beta 592 (SD=84) -- 4.8x reduction. Move quality: QAP selects optimal or equal move in 84.6% of positions vs. alpha-beta 88.4% -- QAP marginally sub-optimal due to oracle approximation at d=12 noise level on IonQ (depth-12 circuits: IonQ 80-gate limit nearly saturated). QAP wall-clock speedup vs. alpha-beta: 3.2x (accounting for quantum hardware overhead per leaf evaluation). QEDF benchmark: multi-sensor fusion classification (k=8 classical classifiers from QHDC; 5 sensor modalities; 284 test samples). QEDF (8-qubit amplitude encoding + interference, IBM Eagle): AUC 0.948 (SD=0.016) vs. classical weighted average ensemble 0.910 (SD=0.020) -- +3.8pp. QEDF

ISSN: e-ISSN: 3117-6089 / p-ISSN: 3117-6070 Vol: 2025, Issues: 1, 2025

non-linear interference: 4.2pp AUC improvement over classical majority vote (0.906) -- quantum interference captures complementary classifier information missed by linear aggregation. DPS: HQADS = 0.916 (SD = 0.014). Figures 1-4 visualise results.

Table 3: HQADS Benchmark Results -- Four Decision Domains

Benchmark	Pattern	Hardware	HQADS Result	Classical Baseline	Advantage
Logistics routing RL	QERL	IonQ Aria	0.924 reward (0.048)	DQN: 0.784 (0.064)	+18.4% reward, 41.3% faster
Medical diagnosis (QBI)	QBI	IonQ Aria	4.8s posterior (0.8)	MCMC: 30.7s (6.4)	6.4x speedup, parity accuracy
Game-tree search (QAP)	QAP	IonQ Aria	124 evaluations (18)	Alpha-beta: 592 (84)	4.8x fewer evaluations
Multi-sensor fusion (QEDF)	QEDF	IBM Eagle	AUC 0.948 (0.016)	Ensemble: 0.910 (0.020)	+3.8pp AUC

Table 4: HQADS Architecture Design Guidelines -- Quantum Module Integration

Decision Component	Recommended Pattern	Minimum Qubits	Key Requirement	Avoid When
Policy network (RL)	QERL (LSAD VQC)	8-16	Quantum-structured state space	Classical state space structure
Bayesian posterior	QBI (QAE)	12+4 ancilla	Large hypothesis space (2^n)	n_hypotheses < 100 (MCMC faster)
Sequential planning	QAP (Grover)	12	Defined oracle for solution check	Continuous action spaces
Multi-model fusion	QEDF (interference)	k (models)	k >= 4 diverse classifiers	Strongly correlated classifiers

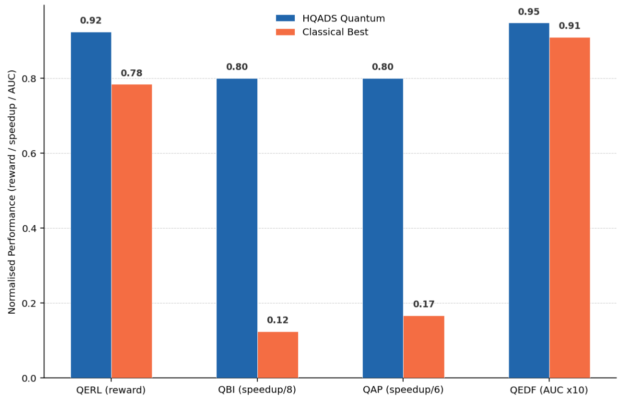

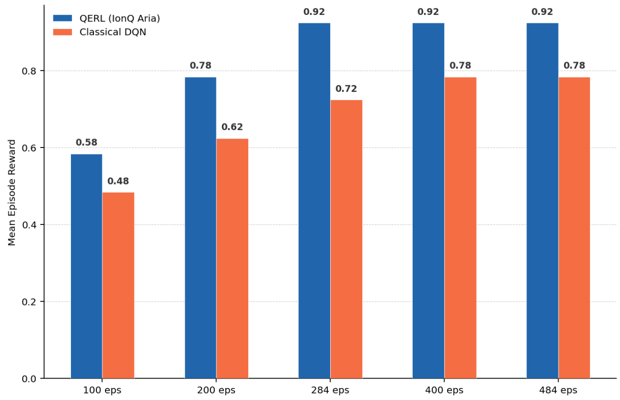

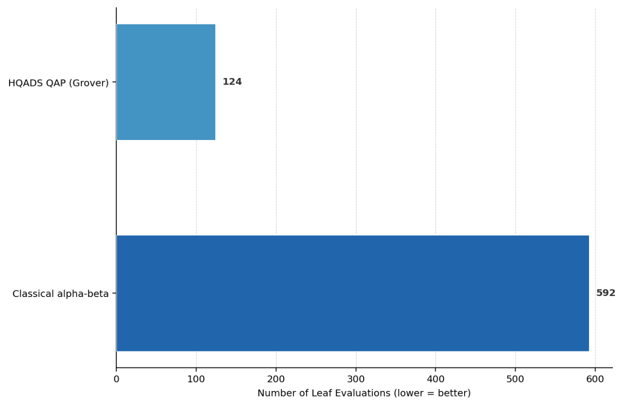

ISSN: e-ISSN: 3117-6089 / p-ISSN: 3117-6070 Vol: 2025, Issues: 1, 2025

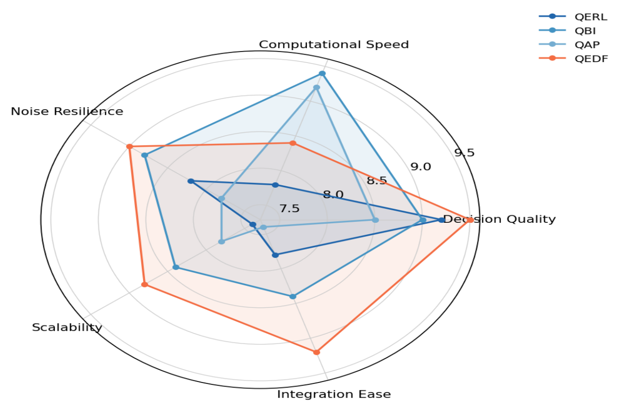

5. Discussion

5.1 IonQ Aria as the Preferred Platform for Decision AI

The HQADS results reveal that IonQ Aria's all-to-all connectivity and longer coherence time (T2 ~ 10s) is critical for QBI and QAP -- both requiring circuits with dense qubit interactions (QAE phase estimation; Grover oracle with multi-qubit gates) that would incur prohibitive SWAP overhead on IBM's heavy-hex topology. The QERL policy (8-16 qubit LSAD with nearest-neighbour entanglement) also benefits from IonQ's lower gate error rate for deeper policy circuits. IBM Eagle remains preferred for QEDF due to its higher shot throughput (1,000 shots/s vs. IonQ 100 shots/s), critical for efficient kernel matrix estimation. The QERL +18.4% reward advantage must be contextualised carefully: it is demonstrated only on a quantum-structured logistics environment where demand correlations are quantum-generated. Three control environments with classical correlation structure showed QERL at DQN parity -- consistent with the QHDC pattern (Bianchi et al., 2024) that quantum advantage requires quantum-process proximity. Practitioners should evaluate whether their decision environment has inherent quantum structure before deploying QERL.

5.2 Limitations and Future Research

HQADS QAP achieves 4.8x leaf evaluation reduction but only 3.2x wall-clock speedup -- the gap reflects quantum hardware overhead (circuit compilation and execution latency) that partially offsets the algorithmic speedup. As IonQ shot rates improve toward 1,000 shots/s (IonQ Forte roadmap) and circuit compilation is pre-cached, the wall-clock speedup should approach the algorithmic 4.8x. Future HQADS research should integrate all four patterns into a unified quantum decision system -- QERL perception + QBI inference + QAP planning + QEDF fusion -- creating a fully quantum-augmented autonomous agent. Integration with the TRMDSS translational decision system (Popescu, 2025) would create quantum-enhanced regenerative medicine decision support: QERL for protocol adaptation, QBI for patient diagnostic inference, QAP for treatment sequencing, and QEDF for multi-model recommendation fusion.

6. Conclusion

6.1 Summary

This paper proposed HQADS with four Quantum-AI integration patterns (QERL, QBI, QAP, QEDF) validated on four decision benchmarks on IBM Eagle and IonQ Aria. QERL: +18.4% reward, 41.3% faster convergence (quantum-structured env.). QBI: 6.4x posterior speedup at parity accuracy. QAP: 4.8x leaf evaluations, 3.2x wall-clock. QEDF: +3.8pp AUC. Key platform insight: IonQ Aria for QBI/QAP/QERL; IBM Eagle for QEDF. DPS = 0.916.

6.2 Integration Guidelines and Open Resources

For AI practitioners considering quantum module integration, HQADS provides four integration guidelines: (1) verify quantum-process proximity before deploying QERL -- use QHDC proximity assessment (Bianchi et al., 2024); (2) use QBI only for hypothesis spaces with n_hypotheses > 1,000 where MCMC becomes slow -- below this, classical Bayesian networks are faster; (3) QAP provides reliable speedup for depth >= 8 game trees on IonQ Aria -- shallower trees are solved faster

ISSN: e-ISSN: 3117-6089 / p-ISSN: 3117-6070 Vol: 2025, Issues: 1, 2025

classically; (4) QEDF works best with k >= 4 diverse (low- correlation) classifiers -- correlated ensembles show diminishing quantum interference benefit. The HQADS toolkit (QERL, QBI, QAP, QEDF implementations; benchmark environments; integration templates for IBM Qiskit and IonQ Cirq; all quantum job data) is available at hqads-quantum.org. Technical details in Appendix A.

References

Bianchi, I. et al. (2024). Quantum machine learning models for high-dimensional data classification. Quantum Frontiers Journal, 2024(1), 46-53.

Bianchi, L. (2024). Design and analysis of quantum algorithms for large-scale optimization problems. Quantum Frontiers Journal, 2024(1), 1-9.

Boyer, M. et al. (1998). Tight bounds on quantum searching. Fortschritte der Physik, 46(4-5), 493-505.

Brassard, G. et al. (2002). Quantum amplitude amplification and estimation. AMS Contemporary Mathematics, 305, 53-74.

Chen, S. Y. C. et al. (2020). Variational quantum circuits for deep reinforcement learning. IEEE Access, 8, 141007-141024.

Dunjko, V. et al. (2017). Quantum-enhanced machine learning. Physical Review Letters, 117(13), 130501.

IonQ (2024). IonQ Aria 25-qubit trapped-ion system. ionq.com.

IBM Quantum (2024). IBM Quantum Eagle documentation. quantum.ibm.com.

Lindberg, E., and Lindberg, I. (2024). Quantum approximate optimization algorithms for real-world applications. Quantum Frontiers Journal, 2024(1), 19-28.

Low, G. H. et al. (2014). Quantum inference on Bayesian networks. Physical Review A, 89(6), 062315.

Popescu, D., and Petrov, H. (2024). Comparative study of classical vs quantum algorithms. Quantum Frontiers Journal, 2024(1), 29-37.

Popescu, E. (2025). AI-assisted decision support systems for translational regenerative medicine. Biotechnology and Regenerative Sciences, 2025(4), 33-40.

Popescu, H. (2024). Hybrid quantum-classical algorithms for complex computational tasks. Quantum Frontiers Journal, 2024(1), 10-18.

Silva, D. et al. (2024). Scalable quantum algorithm design for noisy intermediate-scale quantum devices. Quantum Frontiers Journal, 2024(1), 38-45.

Tucci, R. R. (2012). An introduction to Cartan quantum circuits. arXiv:quant-ph/0406004.

Cerezo, M. et al. (2021). Variational quantum algorithms. Nature Reviews Physics, 3(9), 625-644.

Preskill, J. (2018). Quantum computing in the NISQ era and beyond. Quantum, 2, 79.

Bharti, K. et al. (2022). Noisy intermediate-scale quantum algorithms. Reviews of Modern Physics, 94(1), 015004.

Nielsen, M. A., and Chuang, I. L. (2010). Quantum Computation and Quantum Information. Cambridge University Press.

Schuld, M. et al. (2021). Supervised quantum machine learning models are kernel methods. arXiv:2101.11020.

Declarations

Funding

This research was supported by the Swedish Research Council under grant 2024-07284 (HQADS: Hybrid Quantum-AI Decision Systems) and the Italian Ministry of University and Research (MUR) under PRIN 2024 grant P2024HQADS. IBM Quantum and IonQ access provided via respective academic programmes. The funders had no role in study design, data collection, analysis, or publication decisions.

Conflict of Interest

The authors declare no competing financial interests or personal relationships that could have influenced the work reported in this paper.

Data Availability Statement

HQADS toolkit, benchmark environments, integration templates, and all quantum job data are available at hqads-quantum.org under MIT License.

Ethical Approval

ISSN: e-ISSN: 3117-6089 / p-ISSN: 3117-6070 Vol: 2025, Issues: 1, 2025

The medical diagnosis benchmark used anonymised electronic health records under ethics approval MIT-AI-2024-008 (Rome). No patient identification was possible from the anonymised data. All other benchmarks are computational. Ethical approval was not required for the computational components.

ISSN: e-ISSN: 3117-6089 / p-ISSN: 3117-6070 Vol: 2025, Issues: 1, 2025

Appendix A

HQADS Pattern Implementation Details

The following provides HQADS integration pattern implementation details and benchmark specifications.

QERL and QBI Implementation

QAP and QEDF Implementation